JCI The Journal of Clinical Investigation

Selective inhibition of RANK blocks osteoclast maturation and function and prevents bone loss in mice

Hyunsoo Kim, Han Kyoung Choi, Ji Hye Shin, Kyung Hee Kim, Ji Young Huh, Seung Ah Lee, Chang-Yong Ko, Han-Sung Kim, Hong-In Shin, Hwa Jeong Lee, Daewon Jeong, Nacksung Kim, Yongwon Choi, Soo Young Lee

J Clin Invest. 2009;119(4):813-825. https://doi.org/10.1172/JCI36809.

Research Article **Bone biology**

Regulation of the formation and function of bone-resorbing osteoclasts (OCs) is a key to understanding the pathogenesis of skeletal disorders. Gene-targeting studies have shown that the RANK signaling pathway plays a critical role in OC differentiation and function. Although pharmaceutical blockade of RANK may be a viable strategy for preventing bone destruction, RANK is implicated in multiple biological processes. Recently, a cytoplasmic motif of RANK was identified that may be specifically involved in OC differentiation. Here, we developed a cell-permeable inhibitor termed the *RANK receptor inhibitor* (RRI), which targets this motif. The RRI peptide blocked RANKL-induced OC formation from murine bone marrow–derived macrophages. Furthermore, RRI inhibited the resorptive function of OCs and induced OC apoptosis. Treatment with the peptide impaired downstream signaling of RANK linked to Vav3, Rac1, and Cdc42 and resulted in disruptions of the actin cytoskeleton in differentiated OCs. In addition, RRI blocked inflammation-induced bone destruction and protected against ovariectomy-induced bone loss in mice. These data may be useful in the development of selective therapeutic agents for the treatment of osteoporosis and other bone diseases.

Selective inhibition of RANK blocks osteoclast maturation and function and prevents bone loss in mice

Hyunsoo Kim,[1,2] Han Kyoung Choi,[1] Ji Hye Shin,[1] Kyung Hee Kim,[1] Ji Young Huh,[1] Seung Ah Lee,[1] Chang-Yong Ko,[3] Han-Sung Kim,[3] Hong-In Shin,[4] Hwa Jeong Lee,[5] Daewon Jeong,[6] Nacksung Kim,[7] Yongwon Choi,[8] and Soo Young Lee[1]

[1]Division of Life and Pharmaceutical Sciences, Center for Cell Signaling and Drug Discovery Research, Department of Life Science, College of Natural Sciences, Ewha Womans University, Seoul, Republic of Korea. [2]Nano-Biomaterials Science Laboratory, Division of Applied Life Sciences (BK21), Graduate School of Gyeongsang National University, Jinju, Republic of Korea. [3]Department of Biomedical Engineering, College of Health Science, Institute of Medical Engineering, Yonsei University, Wonju, Republic of Korea. [4]IHBR, Department of Oral Pathology, School of Dentistry, Kyungpook National University, Daegu, Republic of Korea. [5]College of Pharmacy, Ewha Womans University, Seoul, Republic of Korea. [6]Department of Microbiology and the Aging-associated Disease Research Center, Yeungnam University College of Medicine, Daegu, Republic of Korea. [7]Medical Research Center for Gene Regulation, Chonnam National University Medical School, Gwangju, Republic of Korea. [8]Department of Pathology and Laboratory Medicine, University of Pennsylvania School of Medicine, Philadelphia, Pennsylvania, USA.

Regulation of the formation and function of bone-resorbing osteoclasts (OCs) is a key to understanding the pathogenesis of skeletal disorders. Gene-targeting studies have shown that the RANK signaling pathway plays a critical role in OC differentiation and function. Although pharmaceutical blockade of RANK may be a viable strategy for preventing bone destruction, RANK is implicated in multiple biological processes. Recently, a cytoplasmic motif of RANK was identified that may be specifically involved in OC differentiation. Here, we developed a cell-permeable inhibitor termed the *RANK receptor inhibitor* (RRI), which targets this motif. The RRI peptide blocked RANKL-induced OC formation from murine bone marrow–derived macrophages. Furthermore, RRI inhibited the resorptive function of OCs and induced OC apoptosis. Treatment with the peptide impaired downstream signaling of RANK linked to Vav3, Rac1, and Cdc42 and resulted in disruptions of the actin cytoskeleton in differentiated OCs. In addition, RRI blocked inflammation-induced bone destruction and protected against ovariectomy-induced bone loss in mice. These data may be useful in the development of selective therapeutic agents for the treatment of osteoporosis and other bone diseases.

Introduction

Osteoclasts (OCs) are large multinucleated cells (MNCs) that are unique in their ability to resorb bone. Although their activity is normally integrated with the requirements of skeletal morphogenesis and remodeling, excessive bone resorption is a major pathological factor in chronic inflammatory diseases such as osteoporosis, periodontitis, and arthritis (1–3). It is now clear that the deregulation of immune and inflammatory responses is crucial in initiating the bone destruction that is associated with enhanced net OC formation and function (4–6).

In concert with the macrophage growth factor M-CSF, RANKL supplied by bone-forming osteoblasts (OBs) is essential for the differentiation and maturation of OCs as well as cell survival, fusion, and activation in bones (7, 8). Binding of RANKL to its receptor, RANK, activates receptor oligomerization and recruitment of signaling adaptor molecules such as the TNF receptor–associated factor (TRAF) family of proteins (9). Among the known TRAF family members, TRAF2, TRAF5, and TRAF6 can activate transcription factors such as NF-κB and activator protein-1 (AP-1) that are required for OC differentiation (10). RANK interacts with most of the TRAF family members; however, genetic experiments have shown that TRAF6-deficient mice have severe osteopetrosis, implying that the key signals sent through RANK in OC precursors are mediated by the TRAF6 adapter molecule (11, 12).

Downstream of TRAF6, RANKL signaling in OCs activates PI3K, TGF-β–activated kinase 1 (TAK1), Akt/PKB, and MAPKs, including JNK, ERK, and p38, and subsequently a series of transcription factors including NF-κB, c-Fos, Fra-1, cAMP-responsive element–binding protein (CREB), and nuclear factor of activated T cells, cytoplasmic 1 (NFATc1) (4, 5, 7, 8, 13–15). Of these transcription factors, RANKL specifically induces expression of the NFAT family member NFATc1, which is the master regulator of OC differentiation. This induction is dependent on both the TRAF6–NF-κB and the c-Fos pathways via RANKL-RANK stimulation (4, 16, 17). Consequently, NFATc1 regulates a number of OC-specific genes, such as tartrate-resistant acid phosphatase (*TRAP*), OC-associated receptor (*OSCAR*), cathepsin K, β3 integrin, and calcitonin receptor, in cooperation with other transcription factors such as AP-1, PU.1, and microphthalmia-associated transcription factor (MITF) (4, 16, 18–20). The costimulatory molecule pathway, which is transduced by adaptor molecules containing immunoreceptor tyrosine-based activation motif (ITAM), DAP12, and FcRγ, is another signaling system that is required for osteoclastogenesis (4, 5, 21). This pathway, in cooperation with the RANK-TRAF6–induced signaling pathway, leads to the transcriptional upregulation of NFATc1.

Conflict of interest: The authors have declared that no conflict of interest exists.

Nonstandard abbreviations used: AP-1, activator protein-1; BMM, BM monocyte precursor; μCT, microcomputed tomography; MNC, multinucleated cell; Mt, mutant; NFATc1, nuclear factor of activated T cells, cytoplasmic 1; OB, osteoblast; OC, osteoclast; OVX, ovariectomy, ovariectomized; RRI, RANK receptor inhibitor; TRAF, TNF receptor–associated factor; TRAP, tartrate-resistant acid phosphatase.

Citation for this article: *J. Clin. Invest.* **119**:813–825 (2009). doi:10.1172/JCI36809.

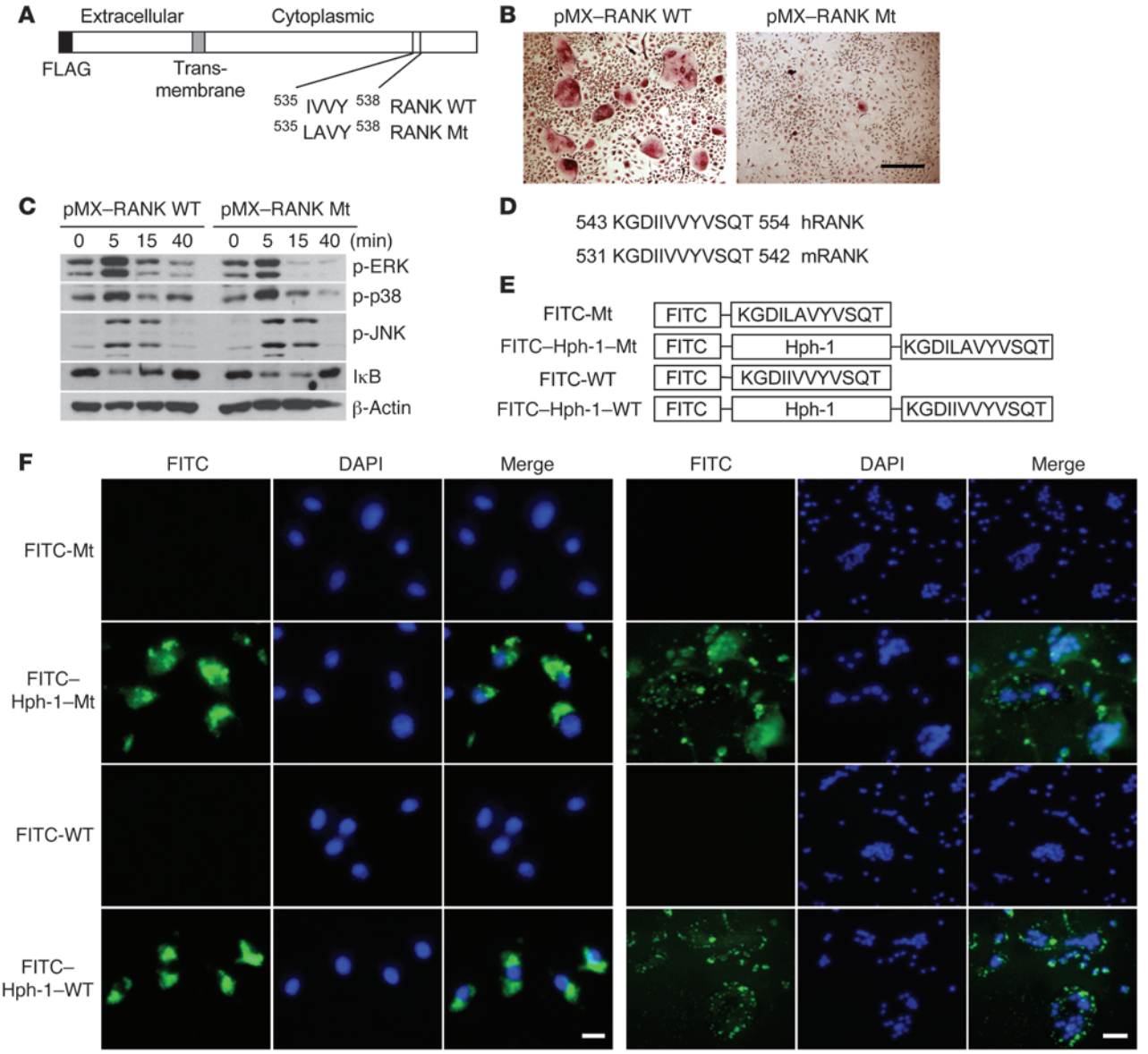

Figure 1
Selection of a RANK inhibitor peptide and transduction of the peptide into BMMs and mature OCs. (**A**) Schematic representation of RANK WT and its Mt (RANK Mt). (**B**) Osteoclastogenesis mediated by RANK WT (pMX–RANK WT) and RANK Mt (pMX–RANK Mt). BMMs were transduced with RANK WT or RANK Mt and stimulated with an anti-FLAG antibody (10 μg/ml). Transduced BMMs were stained for TRAP after 4 days. Scale bar: 200 μm. (**C**) Transduced BMMs were serum starved for 1 hour, stimulated with an anti-FLAG antibody for the indicated period, and analyzed by Western blotting with phospho-ERK, phospho-p38, phospho-JNK, and IκB antibodies. β-actin blots served as loading control. (**D**) Amino acid sequences of human and mouse RANK containing the IVVY motif. These conserved regions were chosen for the design of a RANK inhibitor peptide. (**E**) Structure of the RANK inhibitor peptide conjugated with FITC and Hph-1 protein–transduction domain. (**F**) Transduction of the RANK peptide into BMMs (left 3 columns) and mature OCs (right 3 columns). After 1 hour of incubation with the peptides, intracellular fluorescence was analyzed by fluorescence microscopy. Scale bars: 10 μm (left); 100 μm (right).

Since the RANKL/RANK/TRAF6 axis and NFATc1 are essential for the differentiation of mature OCs, the signaling cascades initiated by RANKL therefore contain several potential antiresorptive therapeutic targets (22). However, the RANKL/RANK system and its numerous downstream protein kinases and transcription factors are not only involved in osteoclastogenic events but also act as a critical mediator of other biological processes, including in the immune system and in mammary gland development (5, 14, 23–25). Therefore, therapies that target these factors might have additional adverse side effects, especially if they are not highly specific (22, 26).

To overcome this issue, we have characterized a signaling pathway that is initiated by a specific motif of RANK (27). While point mutation analyses suggested that this motif might play an important role in OC differentiation in vitro, how it regulates OC formation or whether this motif is also important for the fate of OC in

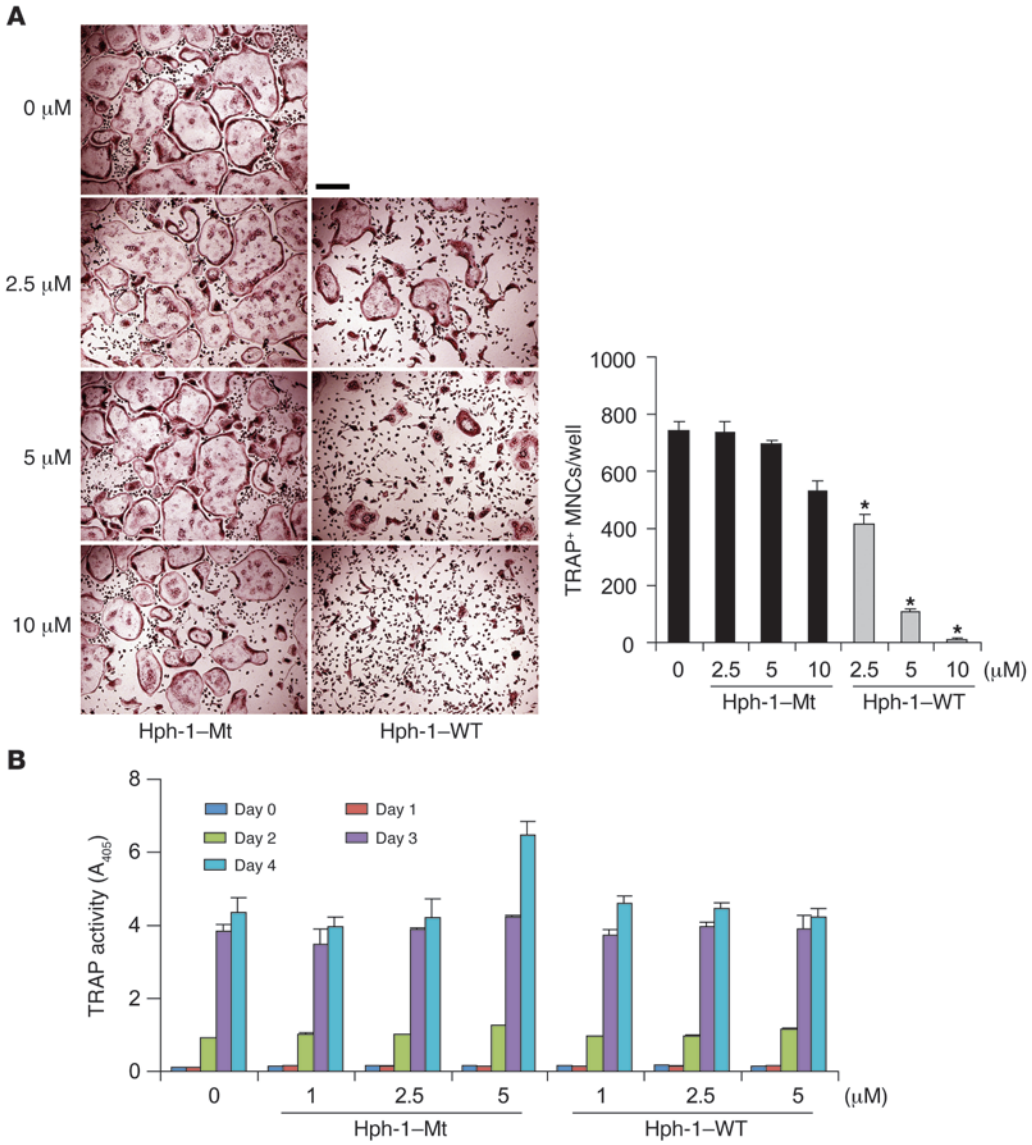

Figure 2
The RRI peptide containing the IVVY motif inhibits RANKL-induced OC formation. (**A**) In vitro differentiation of OCs from BMMs treated with increasing concentrations of RANK WT (Hph-1–WT) and Mt (Hph-1–Mt) peptides, respectively. TRAP$^+$ MNCs containing more than 5 nuclei were counted 4 days after RANKL stimulation. Left panel, TRAP staining. Right panel, number of TRAP$^+$ MNCs. *P < 0.001. Data represent mean ± SD. Scale bar: 200 μm. Of note, Mt peptides at 10 μm had a small effect on reducing the number of OCs, and some experiments did not show any difference. This may be due to a nonspecific effect of the high concentration of cell-permeable peptides. Hence, all the subsequent experiments in this study were carried out at the maximum concentration of 5 μM peptides. (**B**) BMMs were stimulated with RANKL in the presence of varying concentrations of WT and Mt peptides for the indicated time periods. TRAP solution assays were performed. A_{405}, absorbance at 405 nm.

vivo has not been investigated. Our results suggest that an alternative pathway may exist for OC maturation and function that is independent of the RANK/TRAF6 axis as well as NFATc1 induction. Furthermore, the RANK receptor inhibitor (RRI) developed in this study may represent a promising new class of antiresorptive drugs for the treatment of bone diseases that are associated with increased OC formation and activity.

Results

Identification of RANK-initiated signaling that is independent of the TRAF6-mediated pathway. We previously reported that the binding strength between RANK and TRAF6 determines osteoclastogenesis (28). Based on the findings of this study, we determined whether the RANK-TRAF6 interaction is necessary and sufficient to induce osteoclastogenesis. To determine whether there is any TRAF6-independent signaling of the RANK receptor in relation to inducing osteoclastogenesis, RANK WT and RANK mutant (RANK Mt) (Figure 1A), bearing 2 mutations at I535L/V536A, were transduced into OC precursors and their signaling and capacity to induce osteoclastogenesis was tested. When murine BM monocyte precursors (BMMs) overexpressing RANK WT (pMX–RANK WT) were stimulated by cross-linking the introduced FLAG motif to the amino termini using an anti-FLAG antibody, TRAP$^+$ MNCs were formed (Figure 1B). However, the RANK Mt (pMX–RANK Mt) failed to induce OC formation even though the RANK-induced signaling pathways mediated by TRAF6 (7, 9–12) were unaltered (Figure 1, B and C). Furthermore, the RANK Mt did not affect c-Fos expression induced by RANKL (Supplemental Figure 1; supplemental material available online with this article; doi:10.1172/JCI36809DS1). These results suggest that a TRAF6-independent signaling pathway may be induced by RANK stimulation.

We hypothesized that a more selective antiresorptive drug might result from blocking the novel motif of RANK. Therefore, we designed a cell-permeable RRI peptide spanning the RANK IVVY motif that was fused with recently characterized cell-permeable sequences derived from the human transcription factor Hph-1 (Figure 1, D and E) (29). To determine whether Hph-1–WT transduces murine BMMs and OCs, cells were treated with FITC-conjugated

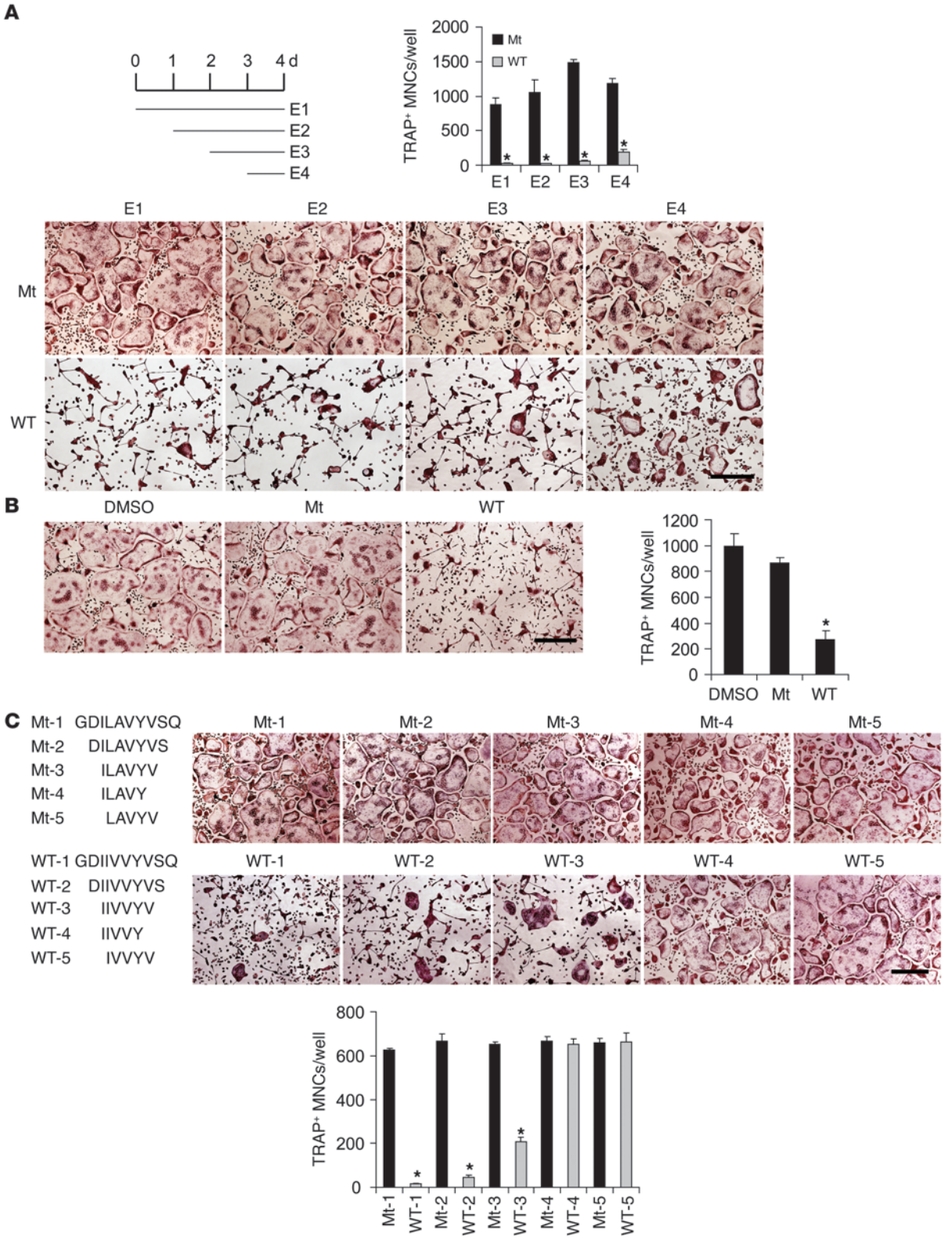
A
0 1 2 3 4 d
E1
E2
E3
E4
TRAP+ MNCs/well
2000
1500
1000
500
0
Mt
WT
E1 E2 E3 E4
Mt
WT
B
DMSO
Mt
WT
1200
1000
800
600
400
200
0
DMSO Mt WT
C
Mt-1 GDILAVYVSQ
Mt-2 DILAVYVS
Mt-3 ILAVYV
Mt-4 ILAVY
Mt-5 LAVYV
WT-1 GDIIVVYVSQ
WT-2 DIIVVYVS
WT-3 IIVVYV
WT-4 IIVVY
WT-5 IVVYV
Mt-1 Mt-2 Mt-3 Mt-4 Mt-5
WT-1 WT-2 WT-3 WT-4 WT-5
800
600
400
200
0
Mt-1 WT-1 Mt-2 WT-2 Mt-3 WT-3 Mt-4 WT-4 Mt-5 WT-5

Figure 3
The RRI peptide inhibits OC formation at the terminal differentiation stage. (**A**) BMMs were cultured for 4 days in M-CSF and RANKL and stained for TRAP activity. Duration of exposure to the peptides in days (left panel) and TRAP-stained OCs (bottom panel). Number of TRAP$^+$ MNCs (right panel). Data are representative of at least 3 experiments. (**B**) Effect of the peptide on pre-OCs fusion. Pre-OCs isolated by coculture of BM cells with OBs for 6 days. Purified pre-OCs were induced to fuse for 24 hours under M-CSF and RANKL treatment in the presence of either WT or Mt peptides. Cells were stained for TRAP (left panel). Number of counted TRAP$^+$ MNCs (right panel). (**C**) Determination of the minimal inhibitory sequences of RANK. Sequences of the RANK inhibitors (WT-1 to WT-5) and control peptides (Mt-1 to Mt-5) (left panel). TRAP-stained OCs (right panel) incubated with each inhibitor (5 μM) and control peptide (5 μM) conjugated with Hph-1 protein transduction domain. Number of TRAP$^+$ MNCs (bottom panel). All data represent mean ± SD. *$P < 0.001$. Scale bars: 200 μm.

Hph-1 peptides. Nearly 100% of both cells displayed a positive fluorescent signal after 1 hour of incubation, and the peptides were mainly distributed in the cytoplasm; the control peptides, which were not fused to Hph-1, were not observed in the cells (Figure 1F).

Inhibitory effect of the RRI on murine OC formation. To determine whether the WT RRI peptide could inhibit osteoclastogenesis, BMMs cultured in RANKL and M-CSF were incubated with either the WT RRI (Hph-1–WT) or the Mt (Hph-1–Mt) peptides. RANKL-induced OC formation was inhibited by incubation with WT RRI in a dose-dependent manner; however, this was not observed with the Mt peptides (Figure 2A). The formation of large (>100 μm) OCs containing more than 5 nuclei was greatly diminished by treatment with the WT peptide. Interestingly, we observed TRAP$^+$ mononuclear cells or much smaller OCs in WT RRI–treated cells. Moreover, TRAP activity (Figure 2B) and the efficiency of mononuclear pre-OC formation from coculture of primary OBs with BMMs (Supplemental Figure 2A) or stromal cell-free BMM cultures with RANKL and M-CSF (Supplemental Figure 2B) were indistinguishable in both WT and Mt peptide–treated cells, suggesting that the RRI peptide may regulate the formation of large OCs but not differentiation of TRAP to TRAP$^+$ OC precursors. To determine the stage of OC formation at which the WT RRI peptide acts, osteoclastogenic cultures were treated with the RRI peptide for various time periods. Exposure to the peptide during the last day of OC differentiation was necessary and sufficient to inhibit OC formation (Figure 3A), suggesting that the RRI peptide may affect the terminal differentiation stage, i.e., cell-cell fusion of pre-OCs (Figure 3B). In addition, the effect of the RRI peptide on OC formation was not due to a reduction in cell survival, since it had no effect on the cell survival of pre-OCs (Supplemental Figure 3).

To define the minimal scaffold size for RANK inhibition, various peptides were synthesized from the sequence surrounding the IVVY motif and the effect of these different peptides on RANKL-induced OC formation was investigated. The minimal required region of the RRI peptide that effectively inhibited OC formation was WT-3 with the core motif IIVVYV, whereas peptides lacking either the last amino acid, valine (WT-4), or the first amino acid, isoleucine (WT-5), were unable to inhibit the formation of mature OCs (Figure 3C). These results indicate that a minimal peptide composed of 6 amino acids is required for efficient inhibition of OC formation. Further mutation analysis of the core peptide IIVVYV revealed that the first 4 amino acids IIVV are relatively important for the inhibitory action (Supplemental Figure 4).

The RRI peptide blocks neither TRAF6-mediated signaling nor NFATc1 induction. To dissect the underlying mechanisms of WT RRI peptide inhibition of OC formation, the effect of the peptide on RANKL-induced signaling pathways including NF-κB, ERK, p38, JNK, and Akt, which are known to be activated via RANKL-RANK-TRAF6–dependent cascades, was examined (4–7, 11, 12). From this analysis, the peptide was found to not abrogate the protein kinase cascades initiated by RANKL (Figure 4A), which is consistent with the observation that BMMs overexpressing RANK Mt constructs, bearing 2 mutations at I535L/V536A, did not alter the RANKL-induced signaling pathways (Figure 1C). Moreover, the mRNA expression profiles of 24,886 genes during osteoclastogenesis were not affected by the RRI peptide. Expression profiles of representative genes analyzed by GeneChip and RT-PCR are shown in Figure 4B and Supplemental Figure 5A. In addition, no change was detected in the cell-surface expression of RANK (Supplemental Figure 5B). Importantly, there were no significant differences in the inducible levels of necessary and/or sufficient factors, including c-Fos (30), c-Src (31), NFATc1 (16), and TRAF6 (32), for OC formation and function (Figure 4C). Moreover, NFATc1 overexpression did not complement the RRI peptide's inhibitory effects (Supplemental Figure 6). Collectively, these data provide evidence that the later stage of OC formation can be induced by a mechanism that is independent of the RANK-TRAF6 interaction and NFATc1 induction and that does not require gene transcription and new protein synthesis.

The RRI peptide regulates cytoskeleton integrity and OC survival. To determine the functional implications of the RRI peptide in mature OCs, the capacity of mature OCs to resorb mineralized matrix in the presence of the peptide was examined. The resorbed area on dentine slices was greatly reduced by the addition of the WT RRI peptide but not by the addition of the Mt peptide (Figure 5A). These results suggest that WT RRI regulates the function of mature OCs.

To determine how the blockade of RANK by WT RRI regulates OC formation and function, the morphological impact of the peptide on mature OCs was examined. Surprisingly, peptide-treated OCs changed shape from multinucleated giant cells to an irregular or condensed shape with a smaller cell size (Figure 5B). Consistent with this, the formation of an actin ring was severely disrupted in the presence of WT RRI peptide (Figure 5B). These results suggest that the peptide regulates the formation of the actin ring, a cytoskeletal structure that is essential for OC functions such as bone resorption (33). Furthermore, RANKL-induced OC survival was severely impaired by treatment with the WT RRI peptide (Figure 5, C and D). Also, the activity of caspase-3 and -9 increased in OCs treated with the RRI peptide (Figure 5E). Therefore, our results suggest that the maintenance of cytoskeleton integrity initiated by the novel motif of RANK is critical for OC function and survival.

The RRI peptide blocks Vav3 and small GTPase signaling. To further elucidate the underlying mechanism that links the IVVY motif of RANK to cytoskeleton integrity, the IVVY-binding complexes were identified by mixing immobilized IVVY-bearing or Mt peptides with pre-OC cell lysates. Since cytoskeletal organization in the OC is regulated by guanine exchange factors (GEFs) (34, 35), we determined whether the peptide precipitates contained GEFs. Interestingly, Vav3, a Rho GEF, was detected in the precipitates that were pull-downed by the IVVY peptides (Figure 6A). To further confirm the binding, we overexpressed the cytoplasmic

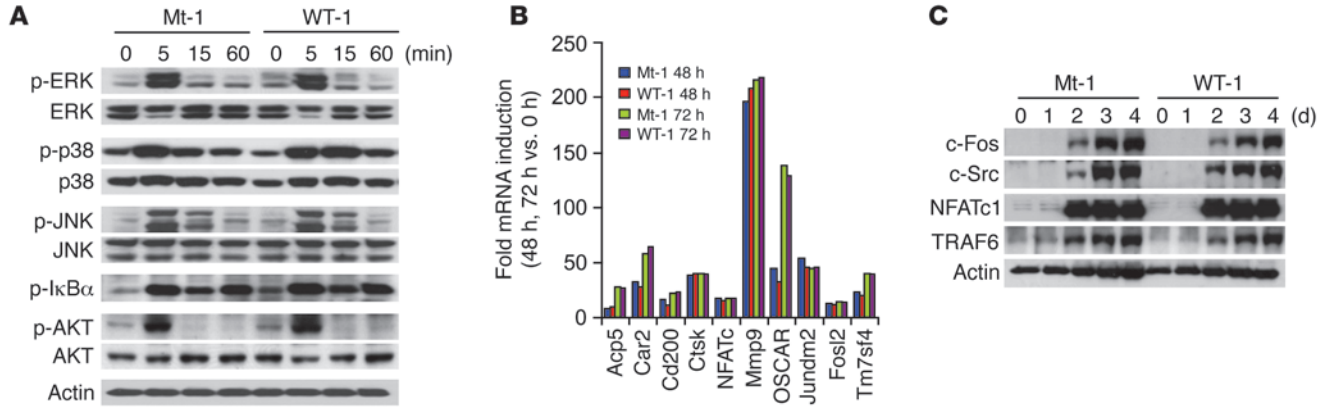

Figure 4

The RRI peptide affects neither the TRAF6-dependent signaling pathways nor RANKL-induced gene expression. (**A**) Effect of the RANK peptide on the RANKL signaling pathways assessed by phosphorylation of ERK, p38, JNK, IκBα, and Akt. Immunoblots were stripped and then reprobed with total ERK, p38, JNK, Akt, and actin as a loading control. (**B**) GeneChip analysis of mRNA expression of RANKL-inducible genes during osteoclastogenesis in the presence of WT-1 and Mt-1 peptides. (**C**) Effect of the RRI peptide on the expression of c-Fos, c-Src, NFATc1, and TRAF6 during osteoclastogenesis.

domain of RANK WT (aa 235–625) and its Mt, which had 2 mutations at I535/V536, and found that Vav3 bound RANK through the IVVY motif (Figure 6B). Consistent with Vav3 binding to RANK, RANKL induced tyrosine phosphorylation of Vav3, which was significantly diminished in WT peptide–treated pre-OCs (Figure 6C). We then determined whether activation of small GTPases is induced downstream of RANKL. From these experiments, RANKL-induced activation of Rac1 or Cdc42 but not RhoA was detected in pre-OCs. However, these activations were severely abrogated by treatment with WT RRI peptides (Figure 6D). Indeed, the increased level of constitutively active Rac1 or Cdc42 but not RhoA complemented the peptide's inhibitory effects (Figure 6E). Since M-CSF stimulation leads to Vav3 and Rac1 activation (35), it would be interesting to see whether the RRI peptide affected M-CSF signaling. Unlike the peptide's effects on RANKL-induced Vav3 and Rac1 activation, there was no significant difference in tyrosine phosphorylation of Vav3 and Rac1 activation stimulated by M-CSF (Supplemental Figure 7A). In addition, the protein kinase cascades initiated by CD40 or IL-1β (Supplemental Figure 7, B and C) and RANKL-induced phosphorylation of c-Src (Supplemental Figure 8) were not abrogated by the RRI peptide. These results collectively suggest that RANK-regulated cytoskeleton integrity through Vav3 and Rac1 and/or Cdc42 pathways may play important roles in OC maturation, function, and survival.

Therapeutic effects of the RRI peptide on inflammation- and ovariectomy-induced bone loss. To investigate the effects of the RRI peptide on the pathological formation of OCs during inflammation, subcutaneous tissue over the periosteum of mouse calvaria was injected with vehicle alone (PBS), RANKL, or LPS together with WT or Mt peptide at 1-day intervals for 5 days with the exception of 1 initial injection of LPS followed by injection with PBS. The extent of bone erosion was notably reduced in WT RRI–treated mice, and the formation of $TRAP^+$ MNCs was greatly suppressed (Figure 7, A and B), suggesting that the RRI peptide can inhibit inflammation-induced bone destruction. Similarly, RANKL-induced OC formation and bone destruction in vivo were blocked by the peptide (Figure 7). The RRI peptide treatment resulted in a decrease in the number of mature OCs but without a concurrent increase in pre-OC numbers in vivo (Figure 7C). Since LPS-induced osteoclastogenesis in vivo is mediated by TNF, which is known to enhance the response of OC precursors at low concentrations of RANKL (36, 37), we evaluated the effect of the RRI peptide on the stimulatory effect of TNF. Consistent with a previous report (38), the stimulatory effect of TNF was observed at a low RANKL dose, and the effect was severely inhibited by the RRI peptide but not the Mt (Supplemental Figure 9).

To test the therapeutic potential of WT RRI peptide on bone loss, we studied the effects of WT RRI peptide on an experimental ovariectomized (OVX) model. Microcomputed tomography (μCT) revealed that mice treated with WT RRI displayed marked increases in bone mass accompanied by a concomitant decrease in the BM cavity space when compared with either OVX or Mt-injected OVX (OVX+Mt-1) mice (Figure 8, A and B). Histology of the proximal tibia showed that the number of $TRAP^+$ cells was increased in OVX or Mt-injected OVX animals, whereas no significant increase in $TRAP^+$ cells was observed in WT-injected (OVX+WT-1) animals (Figure 8, C–E). Thus, these results demonstrate that cell-permeable peptides targeting RANK can provide a new strategy for drug development and may be useful in the treatment of various bone diseases.

The RRI peptide does not affect DC survival and cytokine production by RANKL. OCs differentiate from monocyte/macrophage lineage precursors, which also give rise to macrophages and DCs, key components of the immune system, and M-CSF and RANKL, 2 essential factors for osteoclastogenesis, also regulate cells of the immune system (4, 5). We thus determined whether the RRI peptide interferes with phagocytosis or DC phenotypes and found that the peptide targeting a specific motif of RANK and RANK-Fc (39) affected neither the phagocytic activity of macrophages (Supplemental Figure 10A) nor DC differentiation (Supplemental Figure 10B).

To define selective inhibitory effects of the RRI peptide compared with RANK-Fc on RANKL-RANK signaling, we determined whether the RRI peptide affects cell survival or cytokine production that is promoted by RANKL in DC (39–41). As

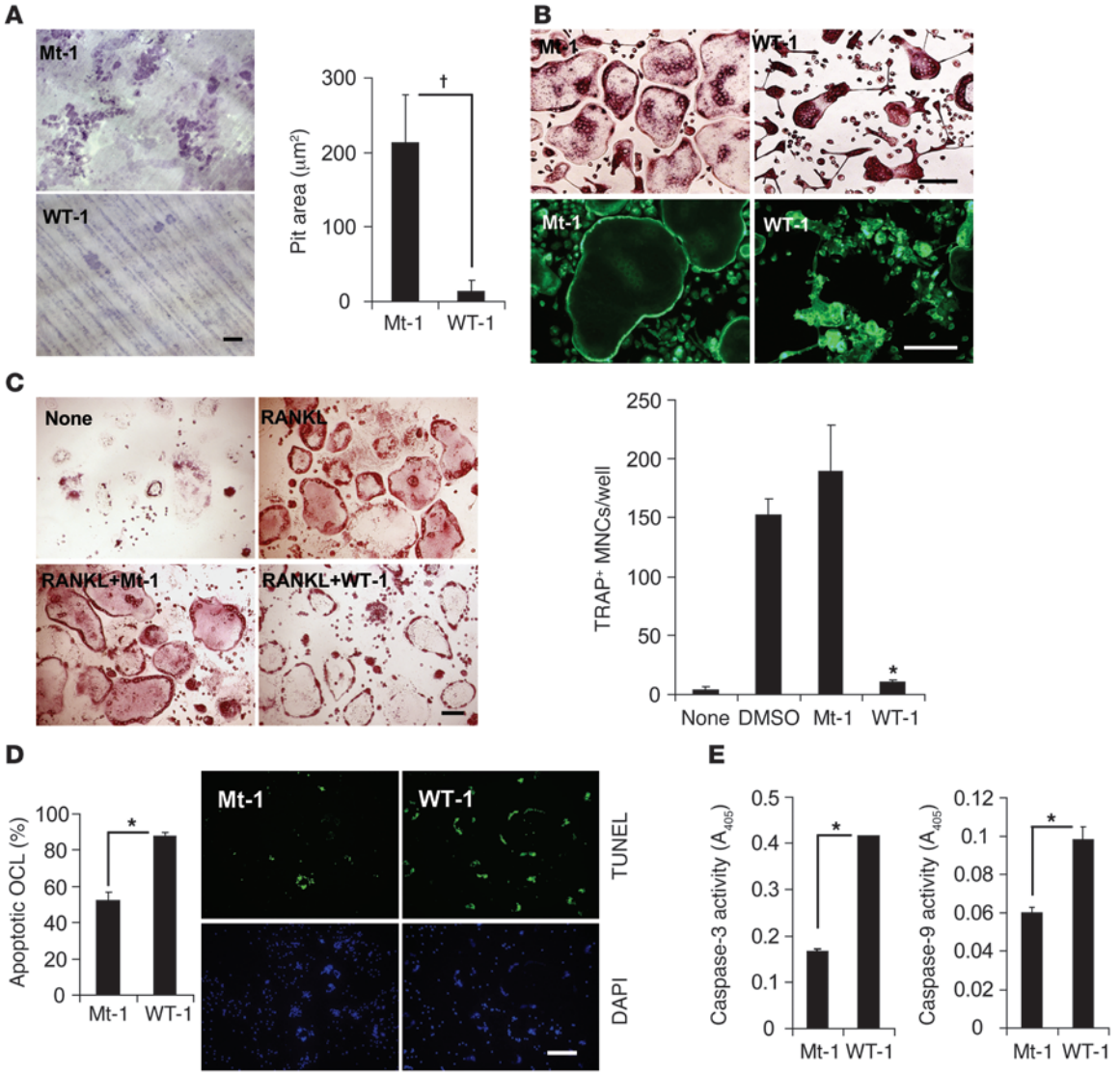

Figure 5

The RRI peptide regulates cytoskeleton integrity and cell survival of OCs. (**A**) Effect of the RANK peptide on pit formation on dentine slices by mature OCs. OCs were generated on dentine slices and stained with hematoxylin for visualization of pit formation. The area of resorption pits was measured with Image-Pro Plus 4.5 (Media Cybernetics). Data represent mean ± SD. Scale bar: 200 μm. (**B**) Mature OCs were generated with RANKL and M-CSF, then treated with the RANK inhibitor (WT-1; 5 μM) or control peptide (Mt-1; 5 μM) for 10 hours. Cells were stained for TRAP (upper panels) and F-actin (lower panels). Data represent mean ± SD. $n = 6$. Scale bar: 100 μm. (**C** and **D**) OC survival assays. BMMs were treated with RANKL and M-CSF for 4 days to promote OC formation. On day 4, the cultures were washed with PBS and then treated as indicated. After 10 hours, the cultures were stained for TRAP (**C**), and a TUNEL assay was performed (**D**). Results are presented as the mean percentage of apoptotic cells. Data represent mean ± SD. $n = 6$. Scale bars: 100 μm. (**E**) Cell lysates from mature OCs were incubated with the caspase-3 (left) or caspase-9 (right) substrate. The release of pNA was measured by absorbance at 405 nm. $^{*}P < 0.001$. $^{\dagger}P < 0.01$. Data represent mean ± SD and are representative of at least 3 experiments.

shown in Figure 9A, blocking the RANKL-RANK interaction with RANK-Fc severely impaired the survival of DC; however, the RRI peptide did not affect DC survival. Moreover, the RRI peptide had no apparent effect on the expression of IL-6 and IL-12p40 in DCs that were induced by RANKL. However, treatment of RANK-Fc resulted in a reduction in IL-6 and IL-12p40 production by more than 80%. Taken together, these data clearly demonstrate that the inhibitory action of the RRI peptide is more selective than that of RANK-Fc.

Discussion

OC differentiation is a multistep process that involves cell proliferation, commitment, fusion, and activation (7, 8). Under pathophysiologic conditions, signaling of the RANKL/RANK/TRAF6 axis in cooperation with costimulatory immunoreceptors leads to the robust induction of NFATc1, which is a necessary and sufficient factor for OC differentiation (4, 5, 15–17). Our studies provide compelling evidence that the RRI peptide can be effectively used to treat bone diseases by targeting a specific process of the

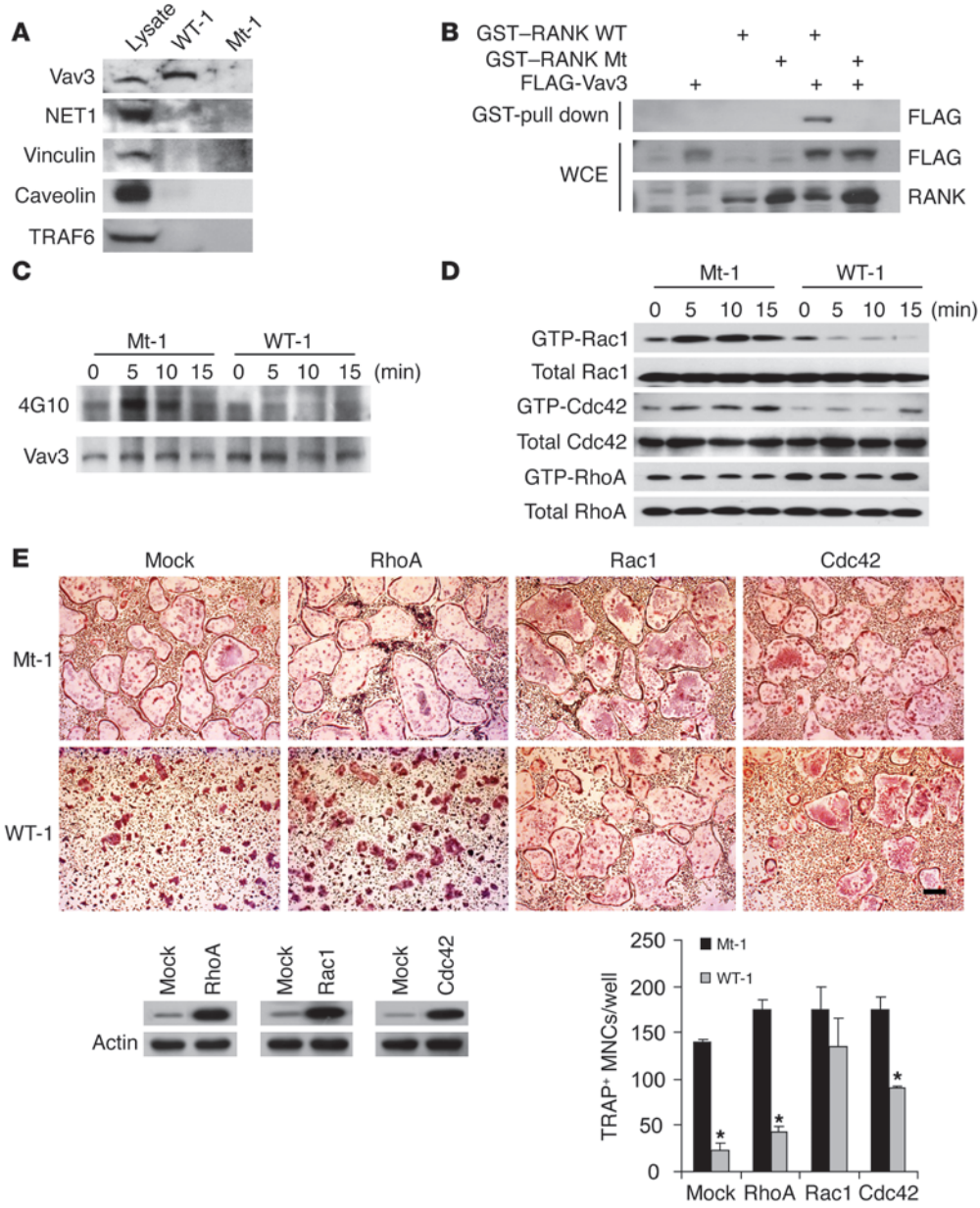

Figure 6
The RRI peptide blocks Vav3 and small GTPase signaling. (**A**) Biotinylated 10-mer peptides were incubated with the pre-OC lysates, and the precipitates were immunoblotted with the indicated antibodies. (**B**) Association of Vav3 with RANK through the IVVY motif. 293T cells were cotransfected with the expression vectors as indicated. Protein complexes were precipitated with glutathione-Sepharose and analyzed by immunoblot analysis using the corresponding antibody. GST–RANK WT, the cytoplasmic tail of RANK WT (aa 235-625) fused to GST; GST–RANK Mt, identical to GST–RANK WT except for 2 mutations at I535L/V536A; FLAG-Vav3, FLAG-tagged Vav3 DNA. (**C**) Vav3 phosphorylation in pre-OCs was assayed in the presence of WT or Mt peptides at the indicated times of RANKL stimulation. A parallel blot with equal loading was used to assess total Vav3 protein. (**D**) Pre-OCs were stimulated with RANKL for the indicated times, and the activated forms of Rac1 and Cdc42 were detected by GST pull-down assays. (**E**) Rescue of TRAP$^+$ MNC formation by retrovirus-mediated expression of constitutive active Rac1 or Cdc42 in the presence of RRI peptides. A representative TRAP staining is shown. TRAP$^+$ MNCs were counted. *P < 0.001. Data represent mean ± SD. Scale bar: 100 μm. Mock, empty vector; RhoA, RhoAV14; Rac1, Rac1V12; Cdc42, Cdc42V12. Rac1, Cdc42, and RhoA expression were confirmed by immunoblot analysis using the corresponding antibody.

RANK signaling pathway. Specifically, the RRI peptide did not abrogate any known protein kinase cascades mediated by TRAF6. Furthermore, induction of NFATc1 itself as well as NFATc1-dependent and -independent osteoclastogenic genes was not changed by peptide treatment. These results suggest that the peptide may target a later stage of OC formation after NFATc1 action. Our in vitro finding supports this scenario in that the RRI peptide did not affect the generation of mononuclear pre-OCs but arrested their further maturation. Regardless of its exact mechanism, we can conclude that this RANK motif is not specifically required for the OC differentiation transcriptional program but is crucial for events after the formation of pre-OCs.

The mechanism regulating the later stage of OC maturation remains largely unknown. Although many molecules including DC-specific transmembrane protein (DC-STAMP), Atp6v0d2, and CD200 receptor were previously implicated in OC fusion (42–44), GeneChip and RT-PCR analyses in our study showed that the RNA levels of these genes were remarkably similar between WT peptide–treated and control peptide–treated cells during the entire course of OC formation. These results suggest that an unidentified maturation process may involve the IVVY motif of RANK.

We also found that the RRI peptide impairs formation of RANKL-induced actin ring, which is known to be essential for bone resorption by activated OCs (45, 46). Consistent with this notion, the peptide-treated OCs exhibited a markedly diminished capacity to excavate bone pits. Although RANK has been described as playing roles in the organization of the actin ring (46, 47), how RANK regulates cytoskeletal integrity toward actin ring formation is still not clear. Our data provide what we believe is the first evidence of the involvement of Vav3 in RANK signaling. Vav3 interacts with the IVVY motif of RANK and is rapidly phosphorylated by RANKL stimulation, which is blocked by the RRI peptide. Since RANK did not interact with Vav3

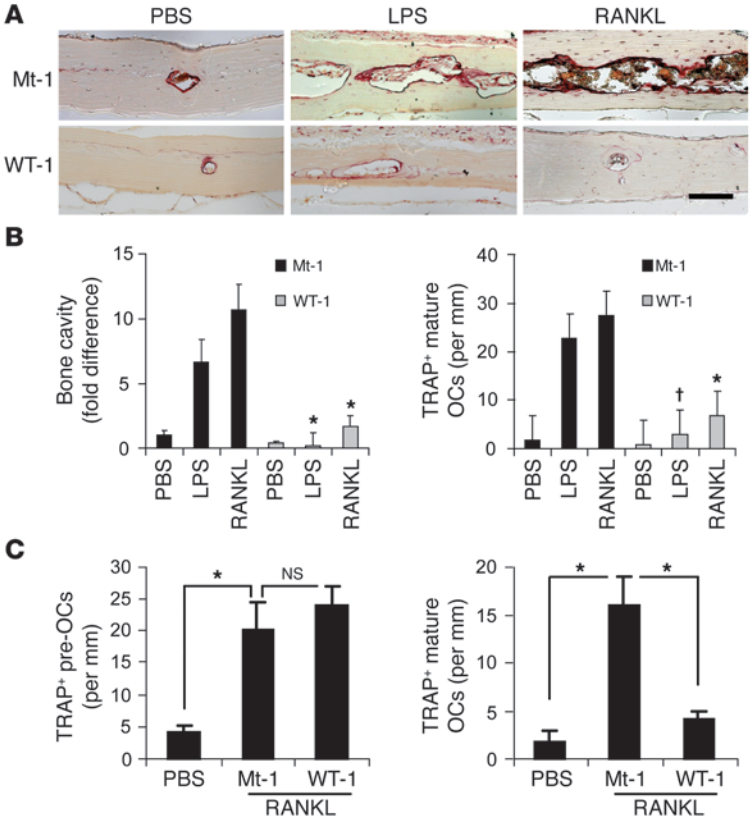

Figure 7
The RRI peptide suppresses LPS- or RANKL-induced OC formation and bone destruction. Inhibition of LPS- or RANKL-induced (12.5 mg LPS or 2 mg RANKL/kg body weight) bone destruction after injection of the RANK inhibitor peptide (20 mg peptide/kg body weight). TRAP staining was performed on sections of calvaria bone (**A**). Scale bar: 100 μm. (**B**) Fold differences of bone cavity (left) and the number of OCs (right) were analyzed. *$P < 0.01$; †$P < 0.05$. Data represent mean ± SD. $n = 7$. (**C**) Effect of the RANK inhibitor peptide on pre-OC formation. Mouse calvaria were injected once with RANKL (2 mg/kg body weight) or PBS, induced for OC formation for 2 days, and then treated with Mt-1 or WT-1 peptide for 2 more days. (**C**) After TRAP staining of calvaria bone, the numbers of pre-OCs (left) and mature OCs (right) were determined. *$P < 0.01$. Data represent mean ± SD. $n = 4$.

in the yeast 2-hybrid assay (data not shown), we hypothesized that RANK may form a complex with Vav3 in OCs through an adaptor molecule. Further studies are necessary to identify an adaptor molecule that directly interacts with RANK via the IVVY motif. In addition, we found that the peptide can inhibit RANKL-induced small GTPases Rac1 and Cdc42 activation but not RhoA. This observation is consistent with the ability of a constitutively active form of Rac1 and Cdc42 but not RhoA to rescue OC cytoskeletal disruption caused by the peptide. In keeping with this conclusion, our study delineated the specific pathway involving RANK-Vav3–small GTPases such as Rac1 and Cdc42 following RANKL stimulation. In addition to cytoskeleton defects, the peptide induced cell death in mature OCs. Whether the collapse of the actin ring induced by the peptide may directly influence the survival of OCs remains to be determined.

Here, we have developed an antiresorptive agent using the peptide-transduction system and identified a mechanism that regulates cytoskeleton integrity. We found that the FITC-RRI peptide accumulated in the BM tissue within 2 hours after intramuscular injection (Supplemental Figure 11). In terms of pharmacokinetic profiles, the FITC-RRI peptide was rapidly eliminated in vivo with a $t_{1/2}$ of approximately 20 minutes (Supplemental Figure 12 and Supplemental Table 1). In spite of the poor pharmacodynamics of the RRI peptide, it acts in vivo to protect mice against inflammation- and OVX-induced bone loss. This phenomenon indicates that a more detailed assessment of in vivo delivery and pharmacokinetic profiles of the RRI peptide may lead to the design of effective therapeutic reagents directed against bone diseases.

In summary, we have shown in this study that selective inhibition of a motif in RANK using the RRI peptide blocks RANKL-induced OC maturation and function both in vitro and in vivo by regulating cytoskeleton integrity and survival of OCs. Moreover, we provide evidence that the inhibitory action of the RRI peptide is TRAF6 and NFATc1 independent. The discovery of the RANKL/RANK system and the in-depth characterization of the signaling pathways induced upon RANK activation, including molecules such as TRAF6, NF-κB, and NFATc1, provides an opportunity for targeted inhibition of OCs (22, 26). Although these molecules are attractive targets for therapeutic intervention in bone diseases, they are also involved in normal cellular physiology such as mounting effective immune and other cellular responses (4, 5, 14–15, 22, 48–53). In this regard, unraveling RANK signaling pathways, as was done in this study, will be beneficial for the development of new generations of therapeutics with high efficacy and fewer side effects.

Methods

Peptide synthesis and in vitro transduction of peptides. Cell-permeable peptides with or without conjugation to FITC and biotinylated peptides were synthesized by Peptron. The peptides were purified by preparative reverse-phase HPLC and were more than 95% pure with the expected amino acid composition and mass spectra. Immediately before use, the peptides were dissolved in DMSO to prepare stock solutions that were between 5 and 10 mM. BMMs or mature OCs were incubated with 5 μM FITC-conjugated peptides, and FITC fluorescence was examined by fluorescence microscopy.

Primary cells and cell line. All primary cells used in this study, including BMMs, pre-OCs, mature OCs, primary OBs, macrophages, and DCs, were generated from murine BM precursors of 6- to 8-week-old C57BL/6 mice (The Jackson Laboratory). 293T cells were used for an experiment depicted in Figure 6B.

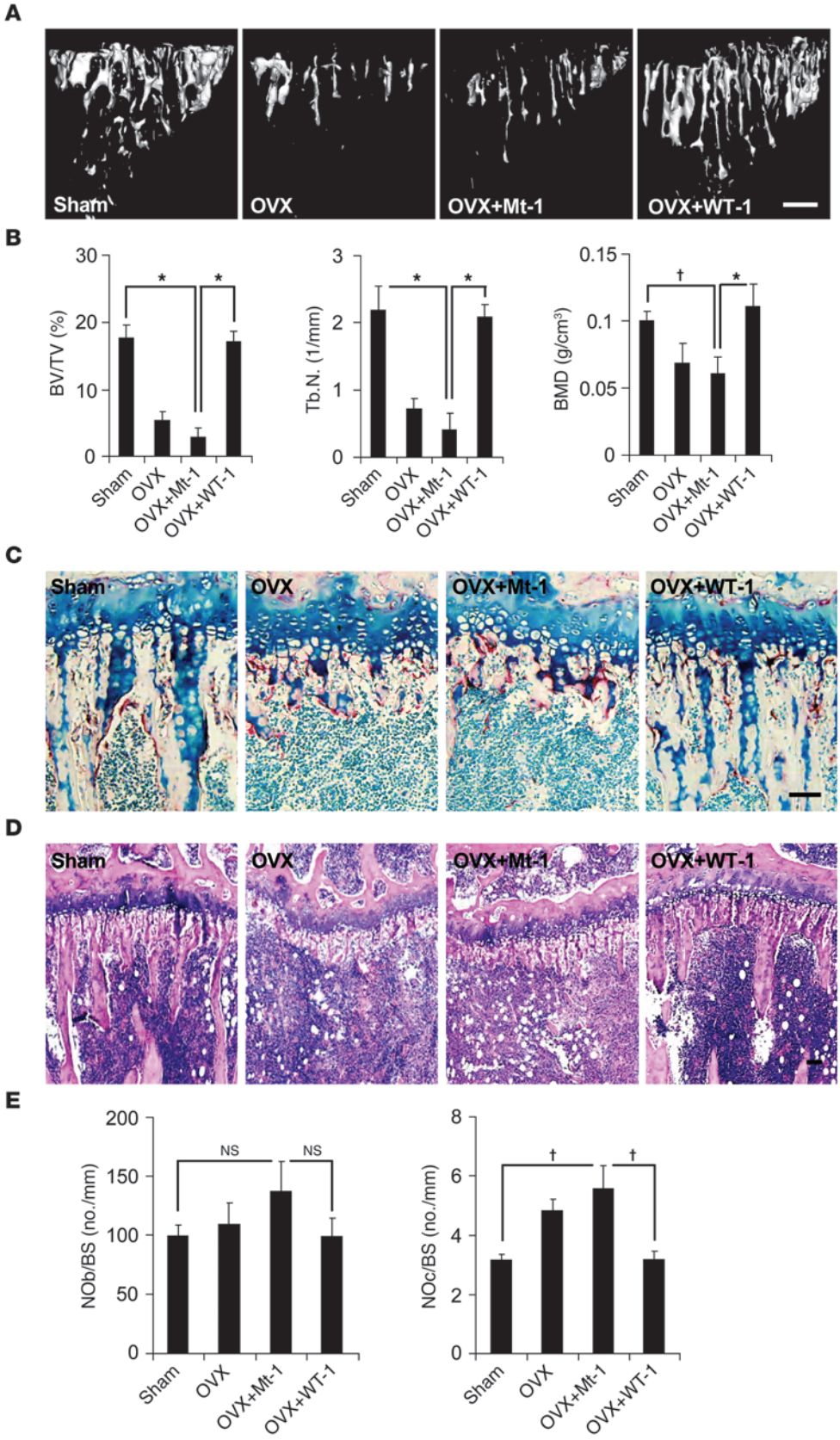

Figure 8

The RRI peptide suppresses OVX-induced OC formation and bone destruction. (**A**) 3D reconstruction of tibiae revealed increased bone mass in OVX mice treated with WT-1 peptide (OVX+WT-1) compared with control mice (OVX+Mt-1). Scale bar: 0.5 mm. (**B**) Tibiae from sham-operated (sham) and OVX (OVX, OVX+Mt-1, and OVX+WT-1) mice were examined by μCT. Histograms represent the 3D trabecular structural parameters in tibiae: bone volume fraction (BV/TV), trabecular number (Tb.N), and bone mineral densities (BMD). $^{*}P < 0.01$, $^{\dagger}P < 0.05$. Data represent mean ± SD. $n = 6$. (**C** and **D**) Histological analysis of the tibiae from OVX mice treated with WT-1 peptide or control Mt-1 peptide. TRAP (**C**) and hematoxylin (**D**) staining. Scale bars: 100 μm. (**E**) Quantification of OC and OB cells. OC number (no.) per bone surface (NOc/BS) and OB number per bone surface (NOb/BS). Data represent mean ± SD. $n = 6$.

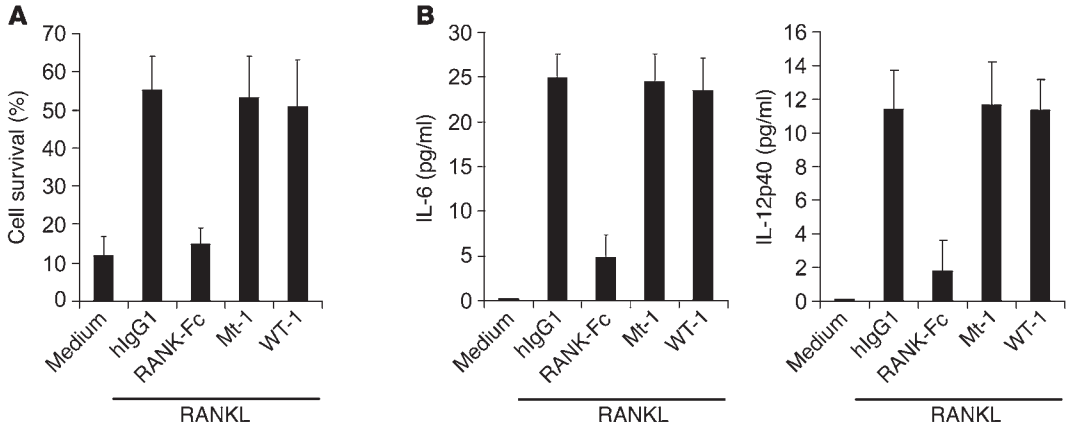

Figure 9
Differential effects of RANK-Fc and RRI peptides on DC survival or cytokine production. (**A**) BM-derived DCs (BMDCs) were cultured with combinations of granulocyte–M-CSF (10 ng/ml), RANKL (500 ng/ml), hIgG1 (10 μg/ml), RANK-Fc (5 μg/ml), and Mt or WT peptides (5 μM) for 72 hours. Cell viability was measured by propidium iodide staining. (**B**) Analysis of IL-6 or IL-12p40 production. BMDCs were left untreated or stimulated as indicated for 12 hours. Culture supernatants were collected, and IL-6 or IL-12p40 production was analyzed by ELISA. Data represent mean ± SD and are representative of at least 3 experiments (**A** and **B**).

GeneChip and protein analysis. For GeneChip analysis (Illumina), total RNA (550 ng) was used for cDNA synthesis by reverse transcription followed by synthesis of biotinylated cRNA using the Ambion Illumina RNA Amplification Kit (Ambion; Applied Biosystems). The labeled cRNA samples were hybridized to the mouse-6 expression bead array according to the manufacturer's instructions (Illumina). For Western blot analysis, equal amounts of cell lysates harvested at the indicated times were subjected to analysis using specific antibodies against IκB, phosphorylated IκB, ERK, phosphorylated ERK, JNK, phosphorylated JNK, p38, phosphorylated p38, Akt, phosphorylated Akt (Cell Signaling Technology), c-Fos, c-Src, NFATc1, TRAF6, NET1 (Santa Cruz Biotechnology Inc.), Vav3 (Upstate; Millipore), Rac1, Cdc42, RhoA (Pierce; Thermo Scientific), and β-actin (Sigma-Aldrich). To assess Vav3 phosphorylation, cell lysates from pre-OCs were immunoprecipitated with a polyclonal antibody specific to Vav3, followed by Western blotting using a 4G10 (Upstate; Millipore) monoclonal antibody. Active Rac1, Cdc42, and RhoA were measured using small GTPase Activation Kits (Thermo Scientific; Pierce) according to the manufacturer's protocol.

In vitro assays for OC formation and function. OCs were prepared from BM cells using a standard method (54). In brief, BM cells were cultured with 30 ng/ml M-CSF (R&D Systems) for 3 days to obtain OC precursor cells of the monocyte/macrophage lineage. The precursor cells were cultured with 30 ng/ml M-CSF and 100 ng/ml RANKL for the indicated time periods. WT or Mt peptides were added at the time of RANKL addition unless otherwise indicated. TRAP assays, F-actin staining, and pit formation were also carried out as previously described (43, 54). Dentin slices for pit formation were kindly provided by M. Takami (Showa University, Tokyo, Japan). $TRAP^+$ cells larger than 100 μm in diameter that contained more than 5 nuclei were counted as $TRAP^+$ MNCs. In some experiments, TRAP solution assays were performed as described (28).

OC fusion assay. Induction of fusion was performed as previously described (55). In brief, purified pre-OCs (1×10^5 cells per well, 200 μl per well, 96-well plates) were cultured with RANKL (100 ng/ml) and M-CSF (30 ng/ml) for 24 hours in the presence of WT or Mt peptides. Cells were stained for TRAP and then examined using a Zeiss Axioplan 2 fluorescence microscope (Zeiss).

Pre-OCs preparation and peptide pull-down assay. Preparation of mononuclear pre-OCs was performed as previously described (28, 43). In brief, mononuclear pre-OCs were prepared by coculturing BMMs (2×10^7 cells per 100-mm dish) with calvarial OBs (2×10^6 cells per 100-mm dish) for 6 days in medium supplemented with 10^{-8} M 1α,25-dihydroxyvitamin D_3 and 10^{-6} M PGE_2. After removal of floating cells, mononuclear cells were harvested from attached cells by gentle pipetting. The purity of pre-OCs in the preparations was approximately 50% as determined by TRAP staining. The pre-OC preparation contained neither OBs (alkaline phosphatase–positive cells) nor MNCs (data not shown). To characterize the RRI peptide–binding protein, about 0.2 mg of biotinylated RRI peptides were bound to 300 μl of an immobilized streptavidin resin (Thermo Scientific; Pierce) and incubated with 1.5 mg of pre-OC lysate at 4°C for 90 minutes; after washing 7 times with 600 μl lysis buffer, the proteins were eluted with 100 μl of sample buffer preheated to 95°C.

Transfection, GST pull down, and immunoblotting. 293T cells were grown under standard conditions (DMEM, 10% FBS, 37°C, 5% CO_2). Cells were replated 24 hours prior to transfection (2×10^6 cells per 100-mm dish) for the interaction assays. The expression vector, GST–RANK WT in pEBG has been described previously (9). We constructed GST–RANK Mt in pEBG by site-directed mutagenesis. The expression vectors were transfected by the calcium phosphate precipitation method. For coexpression-interaction assays, cells were transfected with indicated combinations of expression vectors. The transfectants were lysed, pull-downed by glutathione-Sepharose, and analyzed by immunoblotting under conditions described previously (9).

Retrovirus preparation. A FLAG epitope–tagged cDNA of the RANK Mt and cDNAs for constitutively active forms of small GTPases including Rac1V12, Cdc42V12, and RhoAV14 were cloned into a retroviral vector, pMX-puro. pMX–RANK WT has been previously described (28). Retrovirus packaging was performed by transfecting the plasmids into PLAT-E cells using Lipofectamine 2000 (Invitrogen), and the retroviruses were used to infect BMMs as previously described (43). The pMX-puro vector and PLAT-E cells were kindly provided by T. Kitamura (University of Tokyo, Tokyo, Japan). After infection, BMMs were cultured overnight, detached with trypsin/EDTA, and further cultured with M-CSF (100 ng/ml) and puromycin (2 μg/ml) for 2 days. Puromycin-resistant BMMs were induced to differentiate in the presence of M-CSF (30 ng/ml) and RANKL (100 ng/ml) for an additional 4–5 days.

OC apoptosis assay. Apoptotic cells were detected using the TUNEL assay (ApopTag Plus Fluorescein In Situ Apoptosis Detection Kit; Chemicon, Millipore) according to the manufacturer's instructions. In brief, after BMMs were

differentiated into mature OCs, the cells were placed in fresh medium containing 30 ng/ml M-CSF and 100 ng/ml RANKL and cultured for 10 hours with either WT or Mt RRI peptides. Cells with positive ApopTag labeling were counted and expressed as a percentage of total cell number.

Caspase activity assay. Purified OCs were treated with either WT or Mt RRI peptides for 10 hours. Caspase activity was assayed by a fluorometric kit purchased from R&D Systems. In brief, the cells were washed with ice-cold PBS and lysed in a cell lysis buffer provided in the kit. The caspase-9 (LEHD-pNA) or caspase-3 (DEVE-pNA) substrate was added to the cell lysates in a 96-well plate, and the plates were then incubated for 1 hour. The release of pNA was measured at 405 nm in a microplate reader.

Analysis of disease models. All animal study protocols were approved by the Animal Care Committee of Ewha Laboratory Animal Genomics Center. Models of osteoporosis induced by OVX and an inflammation-induced model of bone loss have been described previously (3, 32). In these models, more than 6 mice were examined in each group. Treatment with WT and Mt peptide commenced 4 days after OVX or sham OVX by intramuscular administration of the peptide in corn oil. We continued the treatment at 4-day intervals for 28 days and terminated the experiment on day 31. Histology and μCT imaging were carried out essentially as previously described (56, 57).

DC survival assays. BM-derived DCs (BMDCs) were from BM suspensions prepared from femurs and tibiae as previously described (40). DCs were left untreated or treated with RANKL (500 ng/ml) in the presence of RANK-Fc (5 μg/ml) (39) or the RRI peptides. DC survival was quantified by measuring cell viability (propidium iodide staining), which was indicated by the fold increase in cell survival compared with that of untreated DCs.

Measurement of cytokines. Mouse IL-6 and IL-12p40 in culture supernatants were measured with ELISA kits from R&D Systems according to the manufacturer's instructions.

Statistics. Data are expressed as mean ± SD from at least 3 independent experiments. Statistical analyses were performed using the 2-tailed Student's *t* test to analyze differences among groups. $P < 0.05$ was considered statistically significant.

Acknowledgments

We thank T. Kitamura for PLAT-E cells and pMX vectors and M. Takami for dentine slices. This work was supported in part by the Korea Science and Engineering Foundation (KOSEF) National Research Laboratory (NRL) Program grant funded by the Korean government (MEST) (R0A-2008-000-20001-0); by KOSEF grants (F104AC010002-07A0301; M1-0641-35-0002; and R13-2005-005-01004-0); and by the National Core Research Facility (NCRC) program (R15-2006-020) of KOSEF through the Center for Cell Signaling and Drug Discovery Research at Ewha Womans University. Y. Choi was supported in part by grants from the NIH (AR053843 and DE019381). H.K. Choi, J.H. Shin, and J.Y. Huh were supported by the second stage of the Brain Korea 21 Project.

Received for publication July 17, 2008, and accepted in revised form January 13, 2009.

Address correspondence to: Soo Young Lee, Division of Life and Pharmaceutical Sciences, Center for Cell Signaling and Drug Discovery Research, Department of Life Science, College of Natural Sciences, Ewha Womans University, Seoul 120-750, Republic of Korea. Phone: 82-2-3277-3770; Fax: 82-2-3277-3760; E-mail: leesy@ewha.ac.kr.

1. Zaidi, M. 2007. Skeletal remodeling in health and disease. *Nat. Med.* **13**:791–801.
2. Mundy, G.R. 2007. Osteoporosis and inflammation. *Nutr. Rev.* **65**:S147–S151.
3. Aoki, K., et al. 2006. A TNF receptor loop peptide mimic blocks RANK ligand–induced signaling, bone resorption, and bone loss. *J. Clin. Invest.* **116**:1525–1534.
4. Takayanagi, H. 2007. Osteoimmunology: shared mechanisms and crosstalk between the immune and bone systems. *Nat. Rev. Immunol.* **7**:292–304.
5. Walsh, M.C., et al. 2006. Osteoimmunology: interplay between the immune system and bone metabolism. *Annu. Rev. Immunol.* **24**:33–63.
6. Boyce, B.F., Schwarz, E.M., and Xing, L. 2006. Osteoclast precursors: cytokine-stimulated immunomodulators of inflammatory bone disease. *Curr. Opin. Rheumatol.* **18**:427–432.
7. Boyle, W.J., Simonet, W.S., and Lacey, D.L. 2003. Osteoclast differentiation and activation. *Nature.* **423**:337–342.
8. Suda, T. 1999. Modulation of osteoclast differentiation and function by the new member of the tumor necrosis factor receptor and ligand families. *Endocr. Rev.* **20**:345–357.
9. Wong, B.R., et al. 1998. The TRAF family of signal transducers mediates NF-κB activation by the TRANCE receptor. *J. Biol. Chem.* **273**:28355–28359.
10. Asagiri, M., and Takayanagi, H. 2007. The molecular understanding of osteoclast differentiation. *Bone.* **40**:251–264.
11. Lomaga, M.A., et al. 1999. TRAF6 deficiency results in osteopetrosis and defective interleukin-1, CD40, and LPS signaling. *Genes Dev.* **13**:1015–1024.
12. Naito, A., et al. 1999. Severe osteopetrosis, defective interleukin-1 signalling and lymph node organogenesis in TRAF6-deficient mice. *Genes Cells.* **4**:353–362.
13. Theill, L.E., Boyle, W.J., and Penninger, J.M. 2002. RANK-L and RANK: T cells, bone loss, and mammalian evolution. *Annu. Rev. Immunol.* **20**:795–823.
14. Walsh, M.C., and Choi, Y. 2003. Biology of the TRANCE axis. *Cytokine Growth Factor Rev.* **14**:251–263.
15. Takayanagi, H. 2005. Mechanistic insight into osteoclast differentiation in osteoimmunology. *J. Mol. Med.* **83**:170–179.
16. Takayanagi, H. 2002. Induction and activation of the transcription factor NFATc1 (NFAT2) integrate RANKL signaling in terminal differentiation of osteoclasts. *Dev. Cell.* **3**:889–901.
17. Asagiri, M., et al. 2005. Autoamplification of NFATc1 expression determines its essential role in bone homeostasis. *J. Exp. Med.* **202**:1261–1269.
18. Crotti, T.N., et al. 2006. NFATc1 regulation of the human β_3 integrin promoter in osteoclast differentiation. *Gene.* **372**:92–102.
19. Kim, Y., et al. 2005. Contribution of NFATc1 to the transcriptional control of immunoreceptor osteoclast-associated receptor but not triggering receptor expressed by myeloid cells-2 during osteoclastogenesis. *J. Biol. Chem.* **280**:32905–32913.
20. Matsumoto, M., et al. 2004. Essential role of p38 mitogen-activated protein kinase in cathepsin K gene expression during osteoclastogenesis through association of NFATc1 and PU.1. *J. Biol. Chem.* **279**:45969–45979.
21. Koga, T., et al. 2004. Costimulatory signals mediated by the ITAM motif cooperate with RANKL for bone homeostasis. *Nature.* **428**:758–763.
22. Tanaka, S. 2007. Signaling axis in osteoclast biology and therapeutic targeting in the RANKL/RANK/OPG system. *Am. J. Nephrol.* **27**:466–478.
23. Josien, R., et al. 2000. TRANCE, a tumor necrosis factor family member, enhances the longevity and adjuvant properties of dendritic cells in vivo. *J. Exp. Med.* **191**:495–502.
24. Loser, K., et al. 2006. Epidermal RANKL controls regulatory T-cell numbers via activation of dendritic cells. *Nat. Med.* **12**:1372–1379.
25. Fata, J.E., et al. 2000. The osteoclast differentiation factor osteoprotegerin-ligand is essential for mammary gland development. *Cell.* **103**:41–50.
26. Sipos, W., Pietschmann, P., and Rauner, M. 2008. Strategies for novel therapeutic approaches targeting cytokines and signaling pathways of osteoclasto- and osteoblastogenesis in the fight against immune-mediated bone and joint diseases. *Curr. Med. Chem.* **15**:127–136.
27. Xu, D., Wang, S., Liu, W., and Feng, X. 2006. A novel receptor activator of NF-κB (RANK) cytoplasmic motif plays an essential role in osteoclastogenesis by committing macrophages to the osteoclast lineage. *J. Biol. Chem.* **281**:4678–4690.
28. Kadono, Y., et al. 2005. Strength of TRAF6 signalling determines osteoclastogenesis. *EMBO Rep.* **6**:171–176.
29. Choi, J.M., et al. 2006. Intranasal delivery of the cytoplasmic domain of CTLA-4 using a novel protein transduction domain prevents allergic inflammation. *Nat. Med.* **12**:574–579.
30. Takayanagi, H., et al. 2002. RANKL maintains bone homeostasis through c-Fos-dependent induction of interferon-β. *Nature.* **416**:744–749.
31. Soriano, P., Montgomery, C., Geske, R., and Bradley, A. 1991. Targeted disruption of the c-src proto-oncogene leads to osteopetrosis in mice. *Cell.* **64**:693–702.
32. Takayanagi, H., et al. 2000. T-cell-mediated regulation of osteoclastogenesis by signalling cross-talk between RANKL and IFN-γ. *Nature.* **408**:600–605.
33. McHugh, K.P., et al. 2000. Mice lacking β_3 integrins are osteosclerotic because of dysfunctional osteoclasts. *J. Clin. Invest.* **105**:433–440.
34. Razzouk, S., Lieberherr, M., and Cournot, G. 1999. Rac-GTPase, OC cytoskeleton and bone resorption. *Eur. J. Cell Biol.* **78**:249–255.
35. Faccio, R., et al. 2005. Vav3 regulates osteoclast

function and bone mass. *Nat. Med.* **11**:284–290.
36. Abu-Amer, Y., Ross, F.P., Edwards, J., and Teitelbaum, S.L. 1999. Lipopolysaccharide-stimulated osteoclastogenesis is mediated by tumor necrosis factor via its P55 receptor. *J. Clin. Invest.* **100**:1557–1565.
37. Lam, J., et al. 2000. TNF-α induces osteoclastogenesis by direct stimulation of macrophages exposed to permissive levels of RANK ligand. *J. Clin. Invest.* **106**:1481–1488.
38. Ochi, S., et al. 2007. Pathological role of osteoclast costimulation in arthritis-induced bone loss. *Proc. Natl. Acad. Sci. U. S. A.* **104**:11394–11399.
39. Josien, R., et al. 1999. TRANCE, a TNF family member, is differentially expressed on T cell subsets and induces cytokine production in dendritic cells. *J. Immunol.* **162**:2562–2568.
40. Wong, B.R., et al. 1997. TRANCE (tumor necrosis factor [TNF]-related activation-induced cytokine), a new TNF family member predominantly expressed in T cells, is a dendritic cell-specific survival factor. *J. Exp. Med.* **186**:2075–2080.
41. Ouaaz, F., et al. 2002. Dendritic cell development and survival require distinct NF-kappaB subunits. *Immunity.* **16**:257–270.
42. Yagi, M., et al. 2005. DC-STAMP is essential for cell-cell fusion in osteoclasts and foreign body giant cells. *J. Exp. Med.* **202**:345–351.
43. Lee, S.H., et al. 2006. v-ATPase V_0 subunit d2–deficient mice exhibit impaired OC fusion and increased bone formation. *Nat. Med.* **12**:1403–1409.
44. Cui, W., et al. 2007. CD200 and its receptor, CD200R, modulate bone mass via the differentiation of osteoclasts. *Proc. Natl. Acad. Sci. U. S. A.* **104**:14436–14441.
45. Burgess, T.L., et al. 1999. The ligand for osteoprotegerin (OPGL) directly activates mature osteoclasts. *J. Cell Biol.* **145**:527–538.
46. Vaananen, H.K., Zao, H., Mulari, M., and Halleen, J.M. 2000. The cell biology of osteoclast function. *J. Cell Sci.* **113**:377–381.
47. Amstrong, A.P., et al. 2002. A RANK/TRAF6-dependent signal transduction pathway is essential for osteoclast cytoskeletal organization and resorptive function. *J. Biol. Chem.* **277**:44347–44356.
48. Boyce, B.F., and Xing, L. 2007. Biology of RANK, RANKL, and osteoprotegerin. *Arthritis Res. Ther.* **9**(Suppl. 1):S1.
49. Cohen, S. 2006. Role of RANK ligand in normal and pathological bone remodeling and the therapeutic potential of novel inhibitory molecules in musculoskeletal diseases. *Arthritis Rheum.* **55**:15–18.
50. Inoue, J., Gohda, J., and Akiyama, T. 2007. Characteristics and biological functions of TRAF6. *Adv. Exp. Med. Biol.* **597**:72–79.
51. Jimi, E., et al. 2004. Selective inhibition of NF-κB blocks osteoclastogenesis and prevents inflammatory bone destruction in vivo. *Nat. Med.* **10**:617–624.
52. Verma, I.M. 2004. Nuclear factor (NF)-κB proteins: therapeutic targets. *Ann. Rheum. Dis.* **63**(Suppl. 2):ii57–ii61.
53. Koga, T., et al. 2005. NFAT and Osterix cooperatively regulate bone formation. *Nat. Med.* **11**:880–885.
54. Suda, T., Jimi, E., Nakamura, I., and Takahashi, N. 1997. Role of 1 α,25-dihydroxyvitamin D3 in osteoclast differentiation and function. *Methods Enzymol.* **282**:223–235.
55. Takami, M., Woo, J.T., and Nagai, K. 1999. Osteoblastic cells induce fusion and activation of osteoclasts through a mechanism of macrophage-colony-stimulating factor production. *Cell Tissue Res.* **298**:327–334.
56. Lee, S.K., et al. 2006. Interleukin-7 influences osteoclast function in vivo but is not a critical factor in ovariectomy-induced bone loss. *J. Bone Miner. Res.* **21**:695–702.
57. Montero, A., et al. 2000. Disruption of the fibroblast growth factor-2 gene results in decreased bone mass and bone formation. *J. Clin. Invest.* **105**:1085–1093.